Spike timing of dendrite-targeting bistratified cells during hippocampal network oscillations *in vivo*

Thomas Klausberger[1], László F Márton[1], Agnes Baude[1,2], J David B Roberts[1], Peter J Magill[1] & Peter Somogyi[1]

Behavior-contingent network oscillations bring about transient, functionally coherent neuronal assemblies in the cerebral cortex, including the hippocampus. Inhibitory input on and close to the soma is believed to phase intrinsic oscillations and output of pyramidal cells, but the function of GABA release to pyramidal cell dendrites remains unknown. We recorded the oscillation-locked spike timing of identified bistratified interneurons in rats. These cells mainly innervated small dendritic shafts of pyramidal cells co-aligned with the glutamatergic Schaffer collateral/commissural input. During theta oscillations, bistratified cells fired at a phase when, on average, pyramidal cell dendrites are most hyperpolarized. Interneurons targeting the perisomatic domain discharge at an earlier phase. During sharp wave–associated ripples, bistratified cells fired with high frequency and in-phase with basket cells, on average 1–2 ms after the discharges in pyramidal cell somata and dendrites. Our results indicate that bistratified cells rhythmically modulate glutamatergic input to the dendrites of pyramidal cells to actively promote the precise input/output transformation during network oscillations.

Spatial memory is encoded in the brain by the firing frequency and spike timing of hippocampal pyramidal cells during network oscillations[1–4]. The firing patterns of pyramidal cells are modulated by a diverse population of GABAergic interneurons[5–9]. Accordingly, perisomatic inhibition has been reported to phase the intrinsic oscillations of pyramidal cells[10] and to provide feed-forward and feed-back inhibition[6,11,12]. The role of dendritic inhibition[13–18] is less clear, especially concerning the modulation of glutamatergic inputs, coincidence detection and dendritic signaling[19–22]. To understand the functions of dendritic GABAergic inputs, it is essential to determine the location and exact timing of GABA release at interneuron synapses on pyramidal cell dendrites *in vivo*.

The firing patterns of hippocampal pyramidal cells and interneurons are often embedded in network oscillations. Theta oscillations (4–10 Hz) are observed in rats during exploration and rapid eye movement (REM) sleep[23], and sharp wave–associated ripples (120–200 Hz) occur during slow-wave sleep (SWS) and consummatory behaviors[24,25]. In a previous study[9], we found a high degree of differential phase specificity in the *in vivo* firing patterns of parvalbumin-expressing basket, axo-axonic and O-LM cells, which make synapses on pyramidal cells at the soma, axon initial segment and distal dendrites, respectively[9]. The synapses from O-LM cells are co-aligned with the entorhinal input to pyramidal cells. The phase difference in the discharges of interneurons releasing GABA to the dendritic and somatic domains of pyramidal cells suggests that, for accurate input-to-output transformation, the relative phases of dendritic and somatic oscillations are governed by distinct GABAergic neurons.

In the present study, we recorded from interneurons that seemed to have different connections from basket, axo-axonic and O-LM cells.

Pyramidal cell dendrites in the stratum radiatum are innervated by the Schaffer collateral/commissural input, and the timing of GABA release to these dendrites may be involved in determining the efficacy of this input[16]. The site and relative phase of this inhibition is particularly interesting because the Schaffer collateral input provides the major glutamatergic drive to the CA1 area during sharp wave–associated ripple oscillations[24]. It also represents a major input during theta oscillations[23]. We determined the exact spike timing and postsynaptic targets of bistratified cells[13,26,27] that make synapses, which are co-aligned with the Schaffer collateral input, onto dendrites in stratum radiatum and stratum oriens.

RESULTS

Spatial relationships of bistratified cells recorded *in vivo*

We recorded the spike timing of seven identified bistratified interneurons in the CA1 area of the hippocampus during theta oscillations (4.1 ± 0.3 Hz, mean $\pm$ s.d.) and sharp wave–associated ripples (118 ± 3 Hz). During theta oscillations, the bistratified cells fired rhythmically on the trough of the theta cycles recorded extracellularly in the pyramidal cell layer (**Fig. 1a**), and bistratified cells also fired with high frequency during sharp wave–associated ripple episodes.

After the extracellular recording, the cells were individually labeled using the juxtacellular labeling method[9,28]. The dendritic trees and representative parts of the axon of all bistratified cells were reconstructed using a drawing tube (**Fig. 1b**). The somata of the bistratified cells were located in stratum pyramidale. The dendrites were generally smooth and were distributed in stratum radiatum and oriens (0.43 ± 0.12 mm mediolateral, 0.58 ± 0.15 mm rostrocaudal, mean $\pm$ s.d.), but avoided stratum lacunosum moleculare; their final

[1]MRC Anatomical Neuropharmacology Unit, Department of Pharmacology, Oxford University, Mansfield Road, Oxford OX1 3TH, UK. [2]CNRS UMR 6150, Faculté de Médecine, IFR Jean Roche, Bd. Pierre Dramard, 13916, Marseille, Cedex 20, France. Correspondence should be addressed to T.K. (thomas.klausberger@pharm.ox.ac.uk).
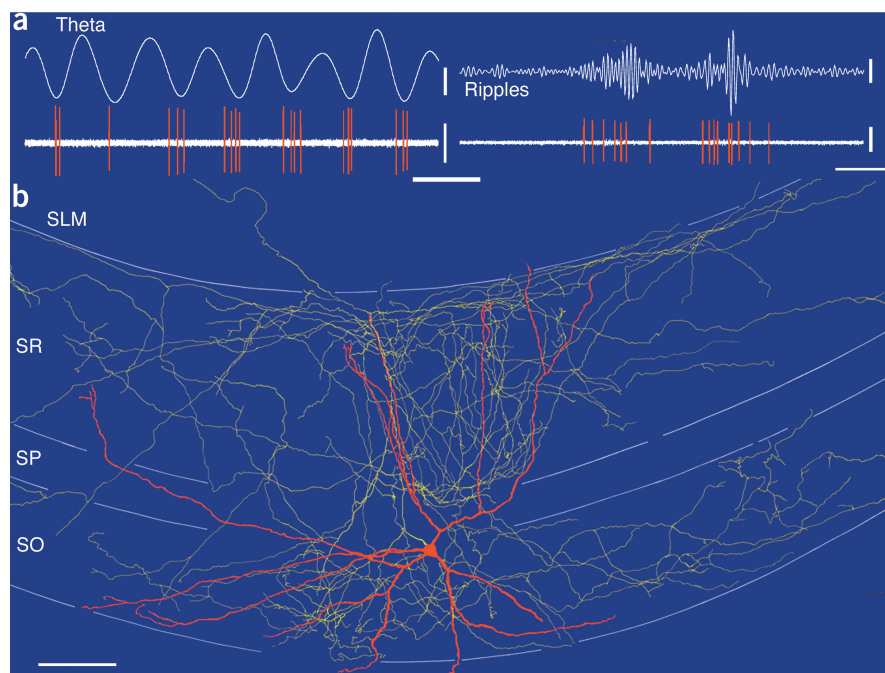
Figure 1 Firing pattern and labeling of a bistratified cell (T92a) in the hippocampus *in vivo*. (**a**) The cell fired rhythmically (left traces) on the trough of the extracellularly recorded theta oscillations (filtered 3–6 Hz; upper trace) and at high frequency (right traces) throughout the whole ripple episodes (filtered 90–140 Hz; upper trace). (**b**) Reconstruction of the recorded and neurobiotin-labeled cell. The soma and dendrites (red) are shown complete; the axon (yellow) is shown from only eight sections of 65 μm thickness for clarity. Note that the axon branches preferentially in stratum radiatum and stratum oriens, but largely avoids stratum pyramidale and lacunosum moleculare. SO, stratum oriens; SP, stratum pyramidale; SR, stratum radiatum; SLM, stratum lacunosum moleculare. Scale bars: (**a**) unit, 0.5 mV; field theta, 0.2 mV, 300 ms; ripples, 0.1 mV, 100 ms; (**b**) 100 μm.

segments were often bent along the boundary. The extent of the axons was 1.15 ± 0.26 mm mediolateral and 1.53 ± 0.38 mm rostrocaudal, and they branched extensively in stratum radiatum and oriens, but were sparse in the pyramidal cell layer and rarely entered stratum lacunosum moleculare (**Fig. 1b**).

The recordings and labeling of five out of seven cells resulted in single-labeled bistratified cells. In two cases during the labeling protocol, the firing of a putative pyramidal cell with distinct spike amplitude and waveform was weakly modulated together with the firing of the interneuron, and a bistratified and an adjacent pyramidal cell were recovered in these cases. Notably, for every filled bistratified cell, one to three faintly neurobiotin-filled interneurons (but no pyramidal cells) could be observed up to a few hundred micrometers away from the labeled cell bodies. These interneurons might have been labeled with neurobiotin via gap junctions[29] because the dendrites of the recorded and of the faintly labeled cells often came in close contact with each other. Alternatively, the faintly filled cells could have innervated the somata of the recorded cells leading to

retrograde labeling[28]. However, the recorded and strongly labeled neurons could be unequivocally identified as bistratified cells, and all seven cells could be reconstructed.

Molecular properties and synaptic output of bistratified cells

The labeled bistratified cells were tested for the expression of various Ca^{2+}-binding proteins, neuropeptides and neurotransmitter-receptors using immunofluorescence microscopy (**Table 1**). All tested bistratified cells were positive for parvalbumin, somatostatin and neuropeptide Y, and their plasma membranes were strongly positive for the $\alpha 1$ subunit of the $GABA_A$ receptor (**Fig. 2**); but no expression of calbindin, calretinin, metabotropic glutamate receptor 1α, or muscarinic acetylcholine receptor type 2 could be detected in their somato-dendritic domains.

Electron-microscopic serial section testing of the postsynaptic targets of bistratified cells in random samples of boutons in stratum oriens, pyramidale and radiatum showed that they made synapses (10 or 11 identified targets per cell tested) predominantly on small or

Table 1 Molecular properties and synaptic targets of bistratified cells

Cell	Expression of proteins and peptides								Number of random postsynaptic targets			
	PV	SM	NPY	GABAR α1	CB	mGluR1α	CR	m2	Pyr. dend. shafts		Pyr. spines	IN
									apical	med./small		
T79e	+	+	n.t.	+	–	n.t.	n.t.	n.t.	1	8	1	0
T83a	+	+	+	+	n.t.	n.t.	–	–	1	8	1	0
T89a	+	+	+	+	–	–	–	–	1	9	0	0
T92a	+	+	+	+	–	–	–	–	0	9	0	1
T96a	+	+	+	n.t.	n.t.	n.t.	n.t.	n.t.	2	7	2	0
T104a	+	+	n.t.	n.t.	–	–	–	n.t.	2	6	1	1
T104b	+	+	+	n.t.	–	–	–	n.t.	0	8	3	0
									10%	76%	11%	3%

PV, parvalbumin; SM, somatostatin; NPY, neuropeptide Y; GABARα1, α1 subunit of the GABA$_A$ receptor; CB, calbindin; mGluR1α, metabotropic glutamate receptor 1α; CR, calretinin; m2, muscarinic acetylcholine receptor type 2; + indicates expression of the respective protein or peptide; – indicates that no signal could be detected in the labeled cell, although nearby cells showed positive signals; n.t. = not tested and indicates that the reaction was either not performed on this cell, or the reaction did not allow a conclusive judgment. Pyr. dend. shafts, dendritic shafts of pyramidal cells; Pyr. spines, dendritic spines of pyramidal cells; IN, dendrites of interneurons.

Figure 2 Fluorescence micrographs showing bistratified cells expressing immunoreactivity for parvalbumin, somatostatin, neuropeptide Y and the α1 subunit of the GABA$_A$ receptor. (**a**) The soma (star) and the dendrite (arrow) of bistratified cell T79e in the pyramidal layer (p) is immunopositive for parvalbumin and the α1 subunit of the GABA$_A$ receptor. Immunoreactivity for the α1 subunit is only weakly present in pyramidal cells (p). Some strongly labeled interneuron dendrites (arrowhead) stand out in stratum oriens. (**b**) Somatostatin and neuropeptide Y immunoreactivity is present in the Golgi apparatus in the soma of bistratified cell T92a (star). Note an unrecorded cell (arrow) expresses neuropeptide Y, but no somatostatin. (**c**) Somatostatin (green) is seen in the boutons of bistratified cell T104a. Colocalization with neurobiotin (red) is indicated by yellow. A part of the axon marked by arrow is shown at higher magnification in the inset. Scale bars (**a**,**b**) 20 μm; (**c**) 10 μm; inset in **c**, 5 μm.

medium size dendritic shafts (76%) of pyramidal cells (**Fig. 3** and **Table 1**). The mean diameter of postsynaptic dendrites was 0.55 ± 0.15 μm ($n = 62$). The main apical dendrites of pyramidal cells (10%, mean diameter of 1.19 ± 0.40 μm, $n = 7$), dendrites of interneurons (3%) and dendritic spines (11%) were rare postsynaptic targets. Dendritic spines were defined as small structures without microtubules receiving one type-I synapse in addition to the bistratified cell synapse. Postsynaptic interneuron dendrites could be distinguished from pyramidal cell dendrites with the criteria that the former (i) receive type-I synapses and (ii) lack spines as established in serial sections. Light microscopic reconstruction of the axons of bistratified cells also showed that they occasionally targeted the soma and proximal dendrites of other interneurons (**Fig. 3c**), confirming previous results[15]. No bistratified cell efferent synapses were found on somata and axon-initial segments of pyramidal cells[15], but the axon of bistratified cells made synapses onto dendrites even in the pyramidal cell layer.

Analysis of spike timing

A visual inspection of the spike timing showed that the firing properties of bistratified cells are intimately related to the ongoing network activity (**Fig. 4**). Bistratified cells fired preferentially on the trough of the theta oscillations recorded extracellularly in the pyramidal cell layer, and the cells also fired with high frequency during sharp wave–associated ripple episodes, often on the ascending phase of the ripples. To quantify these observations, recordings were compared from three different brain states: theta oscillations, non-theta/non-sharp wave periods and sharp wave–associated ripple episodes[8,9]. Bistratified cells fired at significantly different frequencies ($P = 0.0004$, Kruskal-Wallis test) during these brain states, at 5.9 ± 3.0, 0.9 ± 0.1 and 42.8 ± 4.4 Hz (mean ± s.e.m.), respectively (**Table 2**).

A quantitative analysis showed that bistratified cells fired at the trough (1 ± 60°; mean angle ± angular deviation; 0° is at the trough) of the theta oscillations recorded extracellularly in the stratum pyramidale (**Fig. 5a** and **Table 2**). This is similar to another dendrite-targeting interneuron class, the O-LM cells[9], but different from the perisomatically targeting basket (**Fig. 5a**) and axo-axonic cells[9]. In contrast to O-LM cells, which are silenced during ripple episodes[9], bistratified cells fired strongly during these events (**Fig. 5b**). Notably, the bistratified cells did not fire preferentially at the highest amplitude of the ripples like parvalbumin-expressing basket cells, but they fired with similar discharge probability throughout the whole ripple episode. These firing patterns give the bistratified cells a unique physiological signature. In fact, the combined firing behavior during the two oscillations, together with the location of the cells in and close to the pyramidal cell layer, made it possible to predict accurately the identity of this type of cell, even during recording.
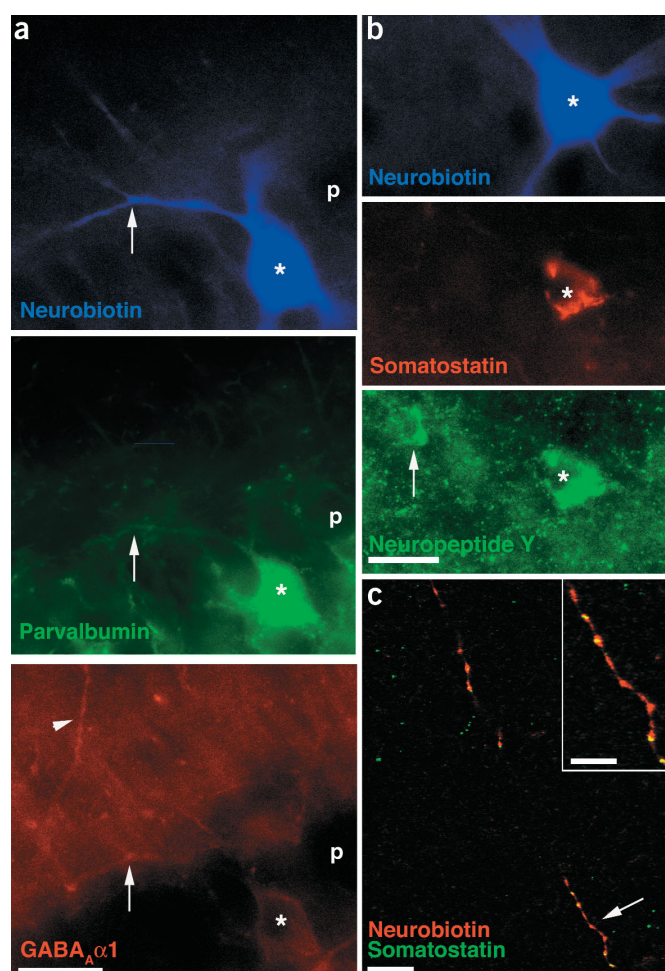
Ripple episodes are of different duration; therefore, to analyze the temporal structure of bistratified cell firing, it is necessary to normalize ripples (**Figs. 4** and **5b**). In some ripple episodes, an increase in the firing of bistratified cells was observed even before the ripples could be detected (threshold was set at 1 s.d. above the mean ripple power) in the local field potential (**Figs. 4** and **5b**). To test whether this was a general feature of bistratified cell activity, we used the first four and last four bins in the normalized ripple episode plots (**Fig. 5b**) to calculate the background firing for every cell. An increase of firing was defined when the cell crossed a threshold set at 2 s.d. above the mean, as calculated from the background firing, for more than one bin. Using the mean length of the ripple episode for each cell, the normalized time of the onset of increased firing was converted into real time. Bistratified cells showed an increase in firing at 64 ± 38 ms (mean ± s.d.) before the beginning of the ripple episode. In contrast, the parvalbumin-expressing basket cells increased their firing only 2 ± 9 ms before the beginning of the ripple episodes. The difference between bistratified and basket cells was significant ($P = 0.003$; Mann-Whitney test). These results indicate that bistratified cells with their dendrites matching the termination zone of the Schaffer collateral/commissural afferents have a low threshold for activation by this pathway and release GABA even before the ripples can be detected in the field potential (that is, before pyramidal cells start to fire).

To determine the spike timing of bistratified cells in relation to pyramidal cell population events during the ripples, we analyzed the phase of the spikes during single ripple cycles (**Fig. 5c**). Bistratified
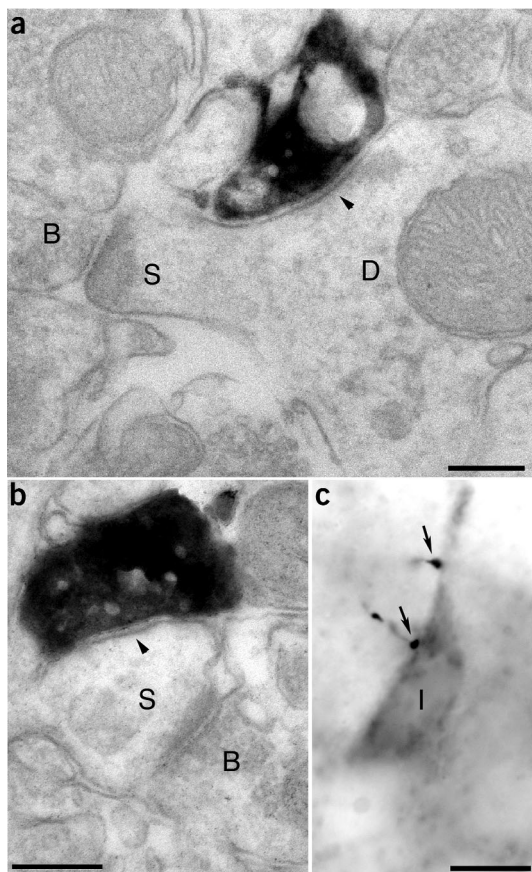
Figure 3 Synaptic targets of bistratified cells. (**a,b**) Electron micrographs of horseradish peroxidase product–labeled boutons (black) in stratum radiatum. (**a**) A bouton of cell T92a makes a type II (GABAergic) synapse (arrowhead) with a dendritic shaft (D) emitting a spine (S), which receives a type-I (presumably glutamatergic) synapse from an unlabeled bouton (B). (**b**) A bouton of cell T104b makes a type-II synapse with a dendritic spine (S), which also receives a type-I synapse from another bouton (B). (**c**) Light micrograph of neurobiotin-labeled boutons (arrows) from bistratified cell T89a targeting the soma and the proximal dendrite of an interneuron (I) in the pyramidal layer. The interneuron was identified by endogenous biotin in its mitochondria. Scale bars: (**a,b**) 0.2 µm; (**c**) 10 µm.

DISCUSSION

We have shown that bistratified cells, which make GABAergic synapses on the dendrites of pyramidal cells, exhibit precise and temporally structured spike timing during behaviorally relevant network oscillations. From our sample of randomly recorded interneurons, the majority of labeled cells targeting pyramidal cells on their dendrites in stratum radiatum and oriens are bistratified cells. Furthermore, bistratified cells are the only cell type shown, as yet, to have a preference for small to medium size dendrites where the majority of CA3 terminals make synapses. The spike timing of bistratified cells is different from previously characterized basket, axo-axonic and O-LM interneurons, which terminate on other domains of the pyramidal cells. Thus, in certain brain states, GABA is released according to different temporal patterns at four distinct domains of pyramidal cells, explaining the need for diverse and precisely wired presynaptic interneurons in the cortical network. The spatiotemporal dynamics of bistratified cells allow them to regulate the structured input/output transformation of pyramidal cells.

It has been suggested that synaptically released GABA could excite pyramidal cells if the resting potential is more hyperpolarized than –68 mV[31,32]. However, the dendrites of active pyramidal cells are strongly depolarized during ripple episodes[30], and the onset of theta oscillations is accompanied by a steady depolarization (magnitude 2–12 mV) of the dendritic membrane[33]. Therefore, at least under the conditions of ripple and theta oscillations in CA1 pyramidal cells, dendritic GABAergic responses are presumably hyperpolarizing. The exact spike timing of the dendrite-targeting bistratified cells suggests that these hyperpolarizing effects might not only shunt dendritic segments and reduce excitation[16,20,34], but might actively structure the

cells fired at the ascending phase (79 ± 92°; mean angle ± angular deviation; 0° is the trough) of the ripples recorded extracellularly from stratum pyramidale. Interestingly, this is similar to the spike timing of parvalbumin-expressing basket cells (**Fig. 5c**), but is different from pyramidal cells, which fire at the trough of the ripple cycles in anesthetized[24] and drug-free[8] animals. In addition, the Na^{+} spikes in the dendrites of pyramidal cells occur at the trough of the ripple cycles[30]. Therefore, bistratified cells fire on average 1–2 ms after the pyramidal cells during ripple episodes. Through synapses co-aligned with the input from Schaffer collaterals in stratum radiatum, bistratified cells implement a GABA-mediated oscillatory input to pyramidal cell dendrites at high temporal precision, which is in phase with the input from parvalbumin-expressing basket cells that modulate the soma of pyramidal cells.

Figure 4 The firing of an identified bistratified cell (T104b) is intimately related to ongoing network oscillations. (**a**) The traces show the local field potential filtered for ripples (90–140 Hz; upper trace), the unfiltered local field potential (dc–220 Hz; middle trace) and the single unit activity of an identified bistratified cell (0.8–5 kHz; lower trace). At the beginning of the trace several ripple episodes occur (asterisks) and the cell fires heavily during these episodes. Then the local field potential changes spontaneously to a regular 4-Hz theta oscillation. Accordingly, the firing of the cell becomes rhythmically phased to the trough of the theta oscillation (gray lines). (**b**) Expanded time scale for ripple episodes shown in **a.** Only the filtered local field potential and the single-unit activity are shown. Note that the cell fires preferentially at the ascending phase of the ripple cycle (gray lines), and the firing of the bistratified cell increases before the ripples can be seen in the local field potential. Vertical scale bars: filtered ripples, 0.2 mV; unfiltered local field potential, 1 mV; single-unit, 1 mV. Horizontal scale bars: (**a**) 1 s; (**b**) 50 ms.
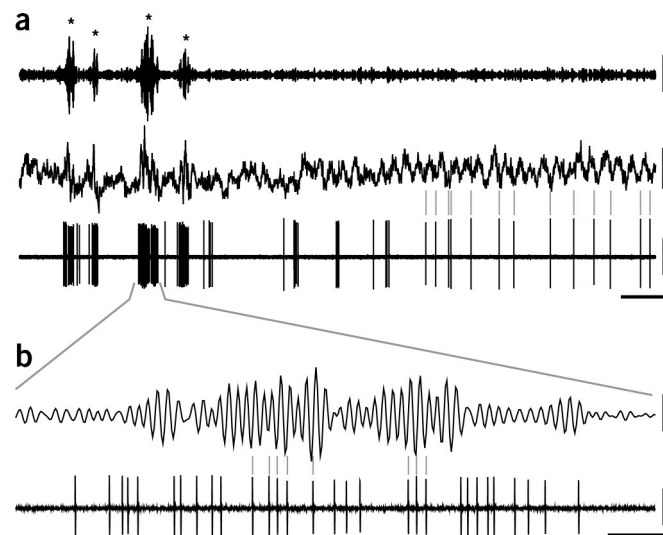
firing of pyramidal cells during theta and ripple oscillations, as discussed below.

During theta oscillations, bistratified cells fire on the trough of the extracellularly recorded theta wave, as do O-LM cells[9], another class of GABAergic cell terminating on more distal dendrites. At this time in the theta cycle, the pyramidal cell dendrites—the postsynaptic targets of these interneurons—are in their relatively hyperpolarized phase[33]. Therefore, bistratified and O-LM cells probably contribute to the hyperpolarization of the overall population of pyramidal cells and phase-modulate the excitatory inputs from the CA3 area of the hippocampus and the entorhinal cortex during theta oscillations.

Interestingly, bistratified cells fire at the phase of the theta cycle when the majority of spikes from pyramidal cells occur. Coincidence of interneuron firing and average pyramidal cell firing has been described in behaving animals as well[8]. This indicates that rhythmic dendritic GABAergic input may have a contrasting effect on cells in different states of activation through an interplay among hyperpolarization, intrinsic properties and synaptic excitation. The rhythmic hyperpolarization during theta oscillations might periodically reduce dendritic excitability in the overall population of pyramidal cells and, through the de-inactivation of voltage-gated cation channels[35], might also facilitate the output of those pyramidal cells which receive strong excitatory input. Such a de-inactivation of channels can promote

burst firing and synaptic plasticity, particularly in those pyramidal cells that are most depolarized by strong excitation. In thalamic relay cells, GABA-mediated hyperpolarization leads to the de-inactivation of a low-threshold Ca^{2+} current, which in turn gives rise to a high-frequency burst of Na^+ action potentials[36,37]. This effect is mediated by T-type Ca^{2+} channels[38] and is involved in burst firing and oscillatory activity during sleep. Interestingly, the required T-type Ca^{2+} channels initiating the burst are also present in the dendrites of hippocampal pyramidal cells[35]. Furthermore, networks of bistratified and O-LM cells provide rhythmic hyperpolarization with a duration of one half of a theta-cycle, which would last for ~70 ms assuming a theta frequency of 7 Hz. This period of hyperpolarization could be sufficient to de-inactivate T-type Ca^{2+} channels[38]. In oscillating thalamic cells, the depolarization, which activates the low-threshold Ca^{2+}

Table 2 Firing properties of bistratified cells

Cell	Discharge frequency (Hz)			Mean theta phase (°) ± angular deviation	Mean ripple phase (°) ± angular deviation
	t	n	s		
T79e	3.1	1.3	30.3	20 ± 48	46 ± 90
T83a	21.7	0.8	41.5	2 ± 63	23 ± 90
T89a	7.1	0.9	41.6	358 ± 64	48 ± 94
T92a	2.1	0.6	28.9	353 ± 35	132 ± 60
T96a	0.5	1.0	46.3	356 ± 42	
T104a	4.7	0.3	52.9	4 ± 50	
T104b	1.9	1.2	57.9	351 ± 42	77 ± 89

t, theta; n, non-theta/non-sharp wave; s, sharp wave-associated ripples.
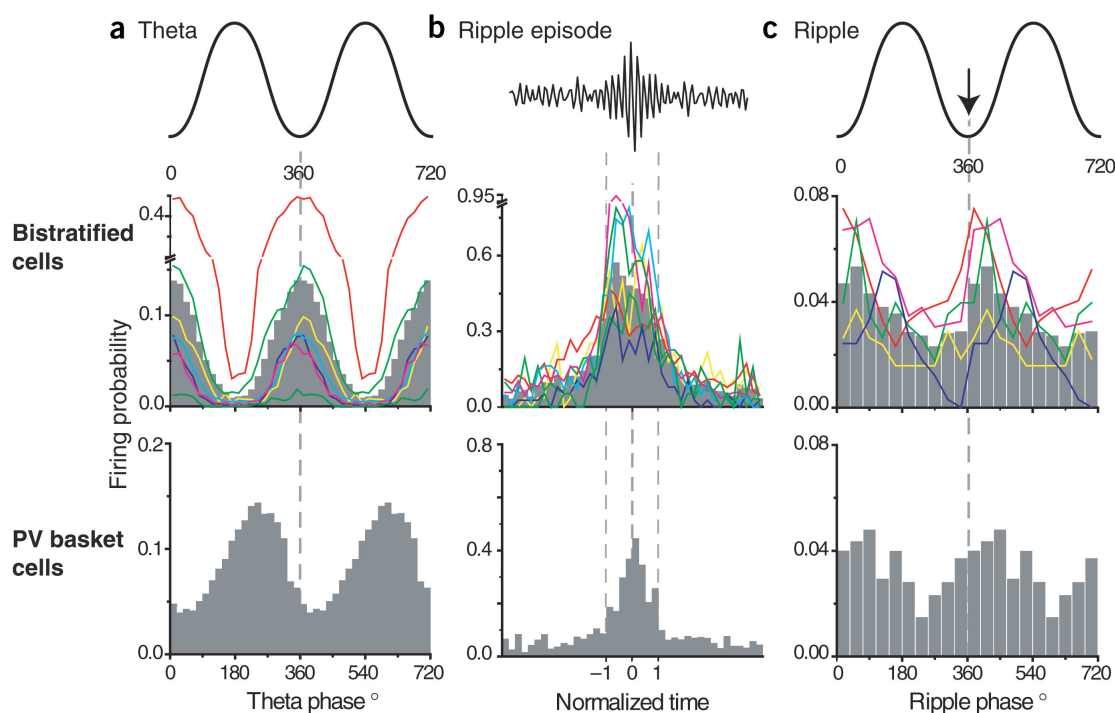

Figure 5 Comparison of the firing patterns of bistratified cells and basket cells during theta oscillations, whole ripple episodes and single ripple cycles (basket cell data for **a** and **b** are taken from ref. 9 with permission). The mean firing probabilities per bin of bistratified and parvalbumin (PV)-expressing basket cells are indicated by gray columns; firing probabilities for single bistratified cells are shown in color. For clarity, the same data is repeated in two theta (**a**) and ripple cycles (**c**), where 0° and 360° mark the troughs of the extracellularly recorded oscillation. (**a**) Bistratified and basket cells fire at different phases during theta oscillations. (**b**) Furthermore, in contrast to basket cells, bistratified cells fire strongly during the whole duration of ripple episodes and increase their firing before the ripples can be detected extracellularly. The start, highest amplitude and end of the normalized ripple episode are marked as −1, 0 and 1, respectively. (**c**) In single ripple cycles, bistratified and basket cells fired simultaneously at the ascending phase of the ripple cycle. The arrow at the trough of the ripple cycle marks the highest probability of spike timing of pyramidal cells[8,24].

spike, is provided by a hyperpolarization-activated cation current (I_h) in the absence of synaptic input. In CA1 pyramidal cells, rhythmic excitatory post synaptic potentials (EPSPs), perhaps together with I_h mediated by HCN1 channels in the distal dendrites[39], are likely to provide the depolarization necessary for activating low-threshold calcium currents. This would result in the activation of other high-threshold currents and subsequently in burst-firing of pyramidal cells. Consistent with this hypothesis, pyramidal place cells start firing exactly on the phase of the theta cycle opposite to the firing of bistratified and O-LM cells[2,23], and they often discharge with a complex spike burst[2,40]. Thus, the dendritic GABAergic input may act in a push-pull manner, increasing the contrast between cells in different functional states; facilitating (push) the output of those receiving strong excitatory inputs as the rat enters the place field by de-inactivating voltage-gated ion channels, while lowering (pull) the firing probability of the majority of pyramidal cells lacking strong excitation by rhythmic hyperpolarization. Although all components required for the above hypothesis of eliciting appropriately timed bursts are present in the hippocampus, the explicit testing of this mechanism requires further work using *in vitro* recording from the dendrites of pyramidal cells.

During sharp wave–associated ripple episodes, bistratified cells fire at high frequency. In fact, these cells increase their firing even before ripples can be detected in the local field potential. Comparison of all cell types recorded so far in the CA1 area[9] suggests that bistratified cells have the lowest threshold for the onset of firing during ripple events. Therefore, bistratified cells are activated most likely by CA3 pyramidal cells during ripple episodes. This further indicates that the excitatory drive to CA1 pyramidal cells from a discharging CA3 pyramid population is constrained by GABA at the dendritic level well before CA1 pyramidal cells begin to fire. The phase of bistratified cell action potentials is similar to that of the parvalbumin-expressing basket cells, indicating that the Schaffer collateral–innervated dendritic domain and the soma receive synchronous inhibitory post-synaptic currents (IPSCs). Therefore, not only the output of the pyramidal cell via the soma[8], but already the glutamatergic input to dendrites is temporally modulated to achieve the high degree of synchrony in the firing of CA1 pyramidal cells.

The prolonged firing of bistratified cells during ripple episodes might result in rhythmic and robust GABA release to small dendrites of pyramidal cells in stratum radiatum, where the majority of glutamatergic terminals from CA3 pyramids provide strong excitation during the ripple episodes, evoking fast dendritic Na$^+$ and slow Ca^{2+} spikes[30]. Together with A-type K$^+$ channels[41], bistratified cell-mediated GABA release might inhibit[16,20,34] or facilitate Ca^{2+} influx into the oblique dendrites of pyramids, depending on the activation state of calcium channels and the magnitude of excitatory drive. The occurrence of fast Na$^+$ spikes in the pyramidal cell dendrites during ripples[30] may have a specific relationship to the spike timing of bistratified cells. Bistratified cells fire with highest probability 1–2 ms after the somatic action potentials of pyramidal cells[8] and after Na$^+$ spikes are detected in pyramidal cell dendrites[30]. Such a phase-locked spike timing during ripples indicates that this GABAergic input might not shunt fast Na$^+$ spikes in pyramidal cell dendrites[22,34]. Instead, the simultaneous firing of bistratified and parvalbumin-expressing basket cells at the ascending phase of the ripple cycle might hyperpolarize pyramidal cells after their firing, as reflected by the consecutive positive peak in the extracellular field potential of the ripple cycle. This hyperpolarization might not only reduce excitation and the probability of pyramidal cell firing[16] during the positive phase of the ripple cycle, but also accelerate the de-inactivation of Na$^+$ channels in the

pyramidal cell dendrites[19,42]. Possible dendritic Na$^+$ spikes in the next ripple cycle can then either back-propagate, if they were initiated in the perisomatic region, or propagate to the soma and more distal dendrites if they were initiated in the dendrites[30,43]. A fast recovery from hyperpolarization, caused by the bistratified cells, together with the de-inactivation of Na$^+$ channels and absence of GABA release from bistratified cells at this time point would promote the firing of pyramidal cells synchronized to the trough of the ripple episode. Therefore, the precisely timed dendritic GABA release might contribute to the retrieval and consolidation of cell assemblies during ripples. The early onset of rhythmic firing of bistratified cells together with their exact spike timing during single ripple cycles suggests that IPSPs produced by bistratified and parvalbumin-expressing basket cells are major contributors to the 120–200 Hz field oscillations seen during sharp waves.

The high frequency and prolonged discharge of bistratified cells during ripple episodes may also lead to the release of neuropeptide Y and somatostatin, which are present in their axon terminals. Neuropeptide Y inhibits glutamate release by acting on Y$_2$ receptors located on the Schaffer collateral terminals[44], whereas somatostatin reduces EPSCs at the Schaffer collateral synapses of pyramidal cells by activating post-synaptic K$^+$ currents[45]. These actions would downregulate the strong excitation evoked by the CA3 pyramids during ripple episodes. This slow feed-forward inhibition mediated by neuropeptides might therefore contribute to the termination of ripple episodes and might help to prevent epileptic oscillations. Indeed, it has been suggested that neuropeptide Y acts as an endogenous anti-epileptic agent[44].

Our results indicate that the restricted location of GABAergic inputs onto pyramidal cell dendrites and their co-alignment with glutamatergic input is supported by a precise timing of the GABA release relative to the activity of the pyramidal cells. The accuracy of inputs from bistratified interneurons in space and time suggests that dendritic GABAergic innervation actively promotes the precision in the firing patterns of pyramidal cells.

METHODS

In vivo **recording and labeling.** All procedures involving experimental animals were carried out in accordance with the Animals (Scientific Procedures) Act, 1986 (UK) and associated procedures. The seven recorded and labeled bistratified cells were obtained from six rats, but overall 62 rats were used to reach this number. Male Sprague-Dawley rats (250–350 g) were anesthetized with urethane (1.25 g per kg of body weight), plus supplemental doses of ketamine and xylazine (20 and 2 mg/kg, respectively) as needed; body temperature was maintained with a heating pad. Neuronal activity in the hippocampus was recorded extracellularly with a glass electrode (18–25 MΩ) filled with 1.5% neurobiotin in 0.5 M NaCl, and the local field potential (LFP) was recorded with the same electrode or a nearby second electrode in the hippocampal CA1 pyramidal cell layer. Single-unit activity (sampling rate 20 kHz) and LFP (sampling rate 800 Hz) were filtered online between 0.8–5 kHz and dc–220 Hz, respectively. Putative interneurons were distinguished from putative pyramidal cells by the lack of complex spike bursts, narrow spike width or sometimes only by a conspicuous firing pattern[8]. We tried to record and label all putative interneurons to avoid sampling only bistratified cells with similar firing patterns. Recorded cells were specifically labeled with neurobiotin using the juxtacellular labeling method[9,28].

Tissue processing and anatomical analysis. The rats were perfused with fixative 4 h after labeling. Immunofluorescence and peroxidase reactions for light and electron microscopy and reconstruction of cells were performed with all necessary controls, as described previously[46]. Antibodies to parvalbumin[47], somatostatin[47], neuropeptide Y[48] and α1 subunit of GABA$_A$ receptor[49] were generous gifts from K. Baimbridge (Department of Physiology, Univ. British Columbia, Canada), A. Buchan (MRC Regulatory Peptide Group, Univ. British Columbia, Canada), J. Polak (Division of Investigative Science, Imperial College London,

UK) and W. Sieghart (Brain Research Institute, Univ. Vienna, Austria), respectively; antibodies to calbindin[46], mGluR1α[47], calretinin[47] and m2 receptor[50] were obtained from Swant, DiaSorin, Swant/Chemicon and Chemicon, respectively. Specificity of these antibodies is discussed in the cited references. In the electron microscopic analysis, all synapses found were photographed, and the nature of the postsynaptic target was determined as described in ref. 15.

Physiological data analysis. The detection of theta, non-theta/non-sharp wave and ripple episodes, the beginning, highest amplitude and end of ripple episodes and the calculation of discharge frequencies of single cells during different brain states was achieved as described previously[9]. To determine the phase relationship between single spikes and the phase of theta or ripple cycles, the troughs of the oscillations were detected in the filtered signal (3–6 or 90–140 Hz). Each spike was assigned to a given phase (bin size 18 or 36°) between the troughs (0 and 360°). For the phase relationship between single cell spikes and ripple cycles, data from cells T104a and T96a were excluded because the large amplitude of the spikes recorded from these cells interfered with the detection of the ripple phase, and no second electrode was present in the hippocampus. Theta and ripple phase was analyzed using circular statistics.

1. O'Keefe, J. & Nadel, L. The Hippocampus as a Cognitive Map (Clarendon Press, Oxford, 1978).
2. O'Keefe, J. & Recce, M.L. Phase relationship between hippocampal place units and the EEG theta rhythm. Hippocampus 3, 317–330 (1993).
3. Wilson, M.A. & McNaughton, B.L. Dynamics of the hippocampal ensemble code for space. Science 261, 1055–1058 (1993).
4. Skaggs, W.E., McNaughton, B.L., Wilson, M.A. & Barnes, C.A. Theta phase precession in hippocampal neuronal populations and the compression of temporal sequences. Hippocampus 6, 149–172 (1996).
5. Andersen, P. & Eccles, J.C. Inhibitory phasing of neuronal discharge. Nature 196, 645–542 (1962).
6. Andersen, P., Eccles, J.C. & Loyning, Y. Recurrent inhibition in the hippocampus with identification of the inhibitory cell and its synapses. Nature 198, 540–542 (1963).
7. Freund, T.F. & Buzsaki, G. Interneurons of the hippocampus. Hippocampus 6, 347–470 (1996).
8. Csicsvari, J., Hirase, H., Czurko, A., Mamiya, A. & Buzsaki, G. Oscillatory coupling of hippocampal pyramidal cells and interneurons in the behaving rat. J. Neurosci. 19, 274–287 (1999).
9. Klausberger T. et al. Brain state– and cell type–specific firing of hippocampal interneurons in vivo. Nature 421, 844–848 (2003).
10. Cobb, S.R., Buhl, E.H., Halasy, K., Paulsen, O. & Somogyi, P. Synchronization of neuronal activity in hippocampus by individual GABAergic interneurons. Nature 378, 75–78 (1995).
11. Buzsaki, G. Feed-forward inhibition in the hippocampal formation. Prog. Neurobiol. 22, 131–153 (1984).
12. Fricker, D. & Miles, R. Interneurons, spike timing, and perception. Neuron 32, 771–774 (2001).
13. Buhl, E.H., Halasy, K. & Somogyi, P. Diverse sources of hippocampal unitary inhibitory postsynaptic potentials and the number of synaptic release sites. Nature 368, 823–828 (1994).
14. McBain, C.J., DiChiara, T.J. & Kauer, J.A. Activation of metabotropic glutamate receptors differentially affects two classes of hippocampal interneurons and potentiates excitatory synaptic transmission. J. Neurosci. 14, 4433–4445 (1994).
15. Halasy, K., Buhl, E.H., Lorinczi, Z., Tamas, G. & Somogyi, P. Synaptic target selectivity and input of GABAergic basket and bistratified interneurons in the CA1 area of the rat hippocampus. Hippocampus 6, 306–329 (1996).
16. Miles, R., Toth, K., Gulyas, A.I., Hajos, N. & Freund T.F. Differences between somatic and dendritic inhibition in the hippocampus. Neuron 16, 815–823 (1996).
17. Szabadics, J., Lorincz, A. & Tamas, G. Beta and gamma frequency synchronization by dendritic gabaergic synapses and gap junctions in a network of cortical interneurons. J. Neurosci. 21, 5824–5831 (2001).
18. Maccaferri, G. & Dingledine, R. Control of feedforward dendritic inhibition by NMDA receptor-dependent spike timing in hippocampal interneurons. J. Neurosci. 22, 5462–5472 (2002).
19. Spruston, N., Schiller, Y., Stuart, G. & Sakmann, B. Activity-dependent action potential invasion and calcium influx into hippocampal CA1 dendrites. Science 268, 297–300 (1995).
20. Magee, J.C. & Johnston, D. A synaptically controlled, associative signal for Hebbian plasticity in hippocampal neurons. Science 275, 209–213 (1997).
21. Markram, H., Lubke, J., Frotscher, M. & Sakmann B. Regulation of synaptic efficacy by coincidence of postsynaptic APs and EPSPs. Science 275, 213–215 (1997).
22. Hausser, M., Spruston, N. & Stuart G.J. Diversity and dynamics of dendritic signaling. Science 290, 739–744 (2000).
23. Buzsaki, G. Theta oscillations in the hippocampus. Neuron 33, 325–340 (2002).
24. Ylinen, A. et al. Sharp wave-associated high-frequency oscillation (200 Hz) in the intact hippocampus: network and intracellular mechanisms. J. Neurosci. 15, 30–46 (1995).
25. Traub, R.D. et al. Axonal gap junctions between principal neurons: a novel source of network oscillations, and perhaps epileptogenesis. Rev. Neurosci. 13, 1–30 (2002).
26. Pawelzik, H., Hughes D.I. & Thomson, A.M. Physiological and morphological diversity of immunocytochemically defined parvalbumin- and cholecystokinin-positive interneurones in CA1 of the adult rat hippocampus. J. Comp. Neurol. 443, 346–367 (2002).
27. Bland, B.H., Konopacki, J. & Dyck, R.H. Relationship between membrane potential oscillations and rhythmic discharges in identified hippocampal theta-related cells. J. Neurophysiol. 88, 3046–3066 (2002).
28. Pinault, D. A novel single-cell staining procedure performed in vivo under electrophysiological control: morpho-functional features of juxtacellularly labeled thalamic cells and other central neurons with biocytin or neurobiotin. J. Neurosci. Meth. 65, 113–136 (1996).
29. Kosaka, T. & Hama, K. Gap junctions between non-pyramidal cell dendrites in the rat hippocampus (CA1 and CA3 regions): a combined Golgi-electron microscopy study. J. Comp. Neurol. 231, 150–161 (1985).
30. Kamondi, A., Acsady, L. & Buzsaki, G. Dendritic spikes are enhanced by cooperative network activity in the intact hippocampus. J. Neurosci. 18, 3919–3928 (1998).
31. Andersen, P., Dingledine, R., Gjerstad L., Langmoen, I.A. & Laursen, A.M. Two different responses of hippocampal pyramidal cells to application of gamma-amino butyric acid. J. Physiol. 305, 279–296 (1980).
32. Gulledge, A.T. & Stuart, G.J. Excitatory actions of GABA in the cortex. Neuron 37, 299–309 (2003).
33. Kamondi, A., Acsady, L., Wang, X.J. & Buzsaki, G. Theta oscillations in somata and dendrites of hippocampal pyramidal cells in vivo: activity-dependent phase-precession of action potentials. Hippocampus 8, 244–261 (1998).
34. Tsubokawa, H. & Ross, W.N. IPSPs modulate spike backpropagation and associated [Ca2+]i changes in the dendrites of hippocampal CA1 pyramidal neurons. J. Neurophysiol. 76, 2896–2906 (1996).
35. Magee, J.C. et al. Subthreshold synaptic activation of voltage-gated Ca^{2+} channels mediates a localized Ca^{2+} influx into the dendrites of hippocampal pyramidal neurons. J. Neurophysiol. 74, 1335–1342 (1995).
36. Jahnsen, H. & Llinas, R. Electrophysiological properties of guinea-pig thalamic neurones: an in vitro study. J. Physiol. 349, 205–226 (1984).
37. Roy, J.P., Clercq, M., Steriade, M. & Deschenes M. Electrophysiology of neurons of lateral thalamic nuclei in cat: mechanisms of long-lasting hyperpolarizations. J. Neurophysiol. 51, 1220–1235 (1984).
38. Crunelli, V. & Leresche N. A role for GABA$_B$ receptors in excitation and inhibition of thalamocortical cells. Trends Neurosci. 14, 16–21 (1991).
39. Lorincz, A., Notomi, T., Tamas, G, Shigemoto, R. & Nusser, Z. Polarized and compartment-dependent distribution of HCN1 in pyramidal cell dendrites. Nat. Neurosci. 5, 1185–1193 (2002).
40. Harris, K.D., Hirase, H., Leinekugel, X., Henze, D.A. & Buzsaki, G. Temporal interaction between single spikes and complex spike bursts in hippocampal pyramidal cells. Neuron 32, 141–149 (2001).
41. Frick, A., Magee, J., Koester, H.J., Migliore, M. & Johnston, D. Normalization of Ca^{2+} signals by small oblique dendrites of CA1 pyramidal neurons. J. Neurosci. 23, 3243–3250 (2003).
42. Colbert, C.M., Magee, J.C., Hoffman, D.A. & Johnston, D. Slow recovery from inactivation of Na$^+$ channels underlies the activity-dependent attenuation of dendritic action potentials in hippocampal CA1 pyramidal neurons. J. Neurosci. 17, 6512–6521 (1997).
43. Chen, W.R., Midtgaard. J. & Shepherd, G.M. Forward and backward propagation of dendritic impulses and their synaptic control in mitral cells. Science 278, 463–467 (1997).
44. Vezzani, A., Sperk, G. & Colmers, W.F. Neuropeptide Y: emerging evidence for a functional role in seizure modulation. Trends Neurosci. 22, 25–30 (1999).
45. Moore, S.D., Madamba, S.G., Joels, M. & Siggins, G.R. Somatostatin augments the M-current in hippocampal neurons. Science 239, 278–280 (1988).
46. Losonczy, A., Zhang, L., Shigemoto, R., Somogyi, P. & Nusser, Z. Cell-type dependence and variability in the short-term plasticity of EPSCs in identified mouse hippocampal interneurones. J. Physiol. 542, 193–210 (2002).
47. Ferraguti, F. et al. Immunolocalisation of metabotrobic glutamate receptor 1? (mGluR1?) in distinct classes of interneuron in the CA1 region of the rat hippocampus. Hippocampus (in press).
48. Allen, Y.S. et al. Neuropeptide Y distribution in the rat brain. Science 221, 877–879 (1983).
49. Zezula, J., Fuchs, K. & Sieghart, W. Separation of alpha 1, alpha 2 and alpha 3 subunits of the GABA$_A$-benzodiazepine receptor complex by immunoaffinity chromatography. Brain Res. 563, 325–328 (1991).
50. Levey, A.I., Edmunds, S.M., Hersch, S.M., Wiley, R.G. & Heilman CJ. Light and electron microscopic study of m2 muscarinic acetylcholine receptor in the basal forebrain of the rat. J. Comp. Neurol. 351, 339–356 (1995).

Corrigendum: Spike timing of dendrite-targeting bistratified cells during hippocampal network oscillations *in vivo*

Thomas Klausberger, László F Márton, Agnes Baude, J David B Roberts, Peter J Magill & Peter Somogyi

In the version of this article initially published, the dose of urethane anesthesia in the Methods section was incorrect. The correct dose should be 1.25 g per kg of body weight. The error has been corrected in the PDF version of the article. The authors regret the error.